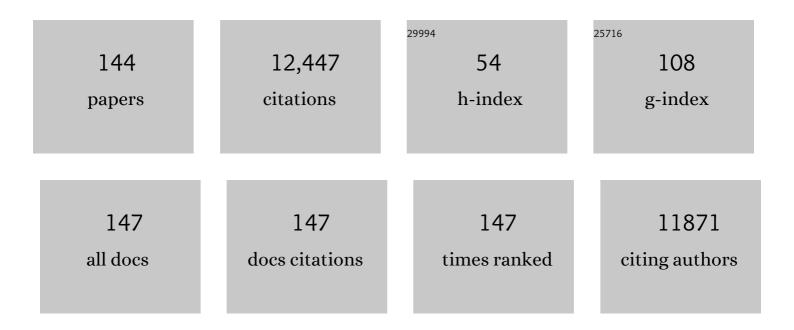
List of Publications by Year in descending order

Source: https://exaly.com/author-pdf/117301/publications.pdf Version: 2024-02-01



#	Article	IF	CITATIONS
1	Coordinatively Unsaturated Al ³⁺ Centers as Binding Sites for Active Catalyst Phases of Platinum on γ-Al ₂ O ₃ . Science, 2009, 325, 1670-1673.	6.0	790
2	Excellent activity and selectivity of Cu-SSZ-13 in the selective catalytic reduction of NOx with NH3. Journal of Catalysis, 2010, 275, 187-190.	3.1	674
3	Enhanced activity and stability of Pt catalysts on functionalized graphene sheets for electrocatalytic oxygen reduction. Electrochemistry Communications, 2009, 11, 954-957.	2.3	615
4	Low-temperature carbon monoxide oxidation catalysed by regenerable atomically dispersed palladium on alumina. Nature Communications, 2014, 5, 4885.	5.8	498
5	Effects of hydrothermal aging on NH3-SCR reaction over Cu/zeolites. Journal of Catalysis, 2012, 287, 203-209.	3.1	438
6	Structure–activity relationships in NH3-SCR over Cu-SSZ-13 as probed by reaction kinetics and EPR studies. Journal of Catalysis, 2013, 300, 20-29.	3.1	409
7	CO ₂ Reduction on Supported Ru/Al ₂ O ₃ Catalysts: Cluster Size Dependence of Product Selectivity. ACS Catalysis, 2013, 3, 2449-2455.	5.5	376
8	Mechanism of CO ₂ Hydrogenation on Pd/Al ₂ O ₃ Catalysts: Kinetics and Transient DRIFTS-MS Studies. ACS Catalysis, 2015, 5, 6337-6349.	5.5	355
9	Simple Synthesis of Functionalized Superparamagnetic Magnetite/Silica Core/Shell Nanoparticles and their Application as Magnetically Separable Highâ€Performance Biocatalysts. Small, 2008, 4, 143-152.	5.2	351
10	Two different cationic positions in Cu-SSZ-13?. Chemical Communications, 2012, 48, 4758.	2.2	350
11	Heterogeneous Catalysis on Atomically Dispersed Supported Metals: CO ₂ Reduction on Multifunctional Pd Catalysts. ACS Catalysis, 2013, 3, 2094-2100.	5.5	310
12	Current Understanding of Cu-Exchanged Chabazite Molecular Sieves for Use as Commercial Diesel Engine DeNOx Catalysts. Topics in Catalysis, 2013, 56, 1441-1459.	1.3	297
13	Effects of Crystallinity on Dilute Acid Hydrolysis of Cellulose by Cellulose Ball-Milling Study. Energy & Fuels, 2006, 20, 807-811.	2.5	258
14	Crosslinked enzyme aggregates in hierarchically-ordered mesoporous silica: A simple and effective method for enzyme stabilization. Biotechnology and Bioengineering, 2007, 96, 210-218.	1.7	187
15	The Effect of Copper Loading on the Selective Catalytic Reduction of Nitric Oxide by Ammonia Over Cu-SSZ-13. Catalysis Letters, 2012, 142, 295-301.	1.4	186
16	Simple Synthesis of Hierarchically Ordered Mesocellular Mesoporous Silica Materials Hosting Crosslinked Enzyme Aggregates. Small, 2005, 1, 744-753.	5.2	184
17	Preparation of biocatalytic nanofibres with high activity and stability via enzyme aggregate coating on polymer nanofibres. Nanotechnology, 2005, 16, S382-S388.	1.3	175
18	Penta-coordinated Al3+ ions as preferential nucleation sites for BaO on γ-Al2O3: An ultra-high-magnetic field 27Al MAS NMR study. Journal of Catalysis, 2007, 251, 189-194.	3.1	173

#	Article	IF	CITATIONS
19	In situ DRIFTS-MS studies on the oxidation of adsorbed NH3 by NO over a Cu-SSZ-13 zeolite. Catalysis Today, 2013, 205, 16-23.	2.2	158
20	Characterization of Cu-SSZ-13 NH3 SCR catalysts: an in situ FTIR study. Physical Chemistry Chemical Physics, 2013, 15, 2368.	1.3	142
21	Preparation of a Magnetically Switchable Bio-electrocatalytic System Employing Cross-linked Enzyme Aggregates in Magnetic Mesocellular Carbon Foam. Angewandte Chemie - International Edition, 2005, 44, 7427-7432.	7.2	137
22	Direct Observation of the Active Center for Methane Dehydroaromatization Using an Ultrahigh Field ⁹⁵ Mo NMR Spectroscopy. Journal of the American Chemical Society, 2008, 130, 3722-3723.	6.6	134
23	Following the movement of Cu ions in a SSZ-13 zeolite during dehydration, reduction and adsorption: A combined in situ TP-XRD, XANES/DRIFTS study. Journal of Catalysis, 2014, 314, 83-93.	3.1	131
24	Synthesis, characterization, and catalytic function of novel highly dispersed tungsten oxide catalysts on mesoporous silica. Journal of Catalysis, 2006, 239, 200-211.	3.1	130
25	Cross-linking Zr-based metal–organic polyhedra via postsynthetic polymerization. Chemical Science, 2017, 8, 7765-7771.	3.7	122
26	NO2Adsorption on BaO/Al2O3:Â The Nature of Nitrate Species. Journal of Physical Chemistry B, 2005, 109, 27-29.	1.2	117
27	A General Strategy to Atomically Dispersed Precious Metal Catalysts for Unravelling Their Catalytic Trends for Oxygen Reduction Reaction. ACS Nano, 2020, 14, 1990-2001.	7.3	116
28	Direct fabrication of enzyme-carrying polymer nanofibers by electrospinning. Journal of Materials Chemistry, 2005, 15, 3241.	6.7	111
29	A Magnetically Separable, Highly Stable Enzyme System Based on Nanocomposites of Enzymes and Magnetic Nanoparticles Shipped in Hierarchically Ordered, Mesocellular, Mesoporous Silica. Small, 2005, 1, 1203-1207.	5.2	106
30	Role of Pentacoordinated Al ³⁺ Ions in the High Temperature Phase Transformation of γ-Al ₂ O ₃ . Journal of Physical Chemistry C, 2008, 112, 9486-9492.	1.5	106
31	(100) facets of Î ³ -Al2O3: The Active Surfaces for Alcohol Dehydration Reactions. Catalysis Letters, 2011, 141, 649-655.	1.4	105
32	The role of H2O in the carbonation of forsterite in supercritical CO2. International Journal of Greenhouse Gas Control, 2011, 5, 1081-1092.	2.3	103
33	Dissecting the steps of CO ₂ reduction: 1. The interaction of CO and CO ₂ with γ-Al ₂ O ₃ : an in situ FTIR study. Physical Chemistry Chemical Physics, 2014, 16, 15117-15125.	1.3	103
34	High-performance and stable photoelectrochemical water splitting cell with organic-photoactive-layer-based photoanode. Nature Communications, 2020, 11, 5509.	5.8	103
35	Unique Role of Anchoring Penta-Coordinated Al ³⁺ Sites in the Sintering of γ-Al ₂ O ₃ -Supported Pt Catalysts. Journal of Physical Chemistry Letters, 2010, 1, 2688-2691.	2.1	101
36	Effect of H2O on the Adsorption of NO2on γ-Al2O3:  an in Situ FTIR/MS Study. Journal of Physical Chemistry C, 2007, 111, 2661-2669.	1.5	97

#	Article	IF	CITATIONS
37	The different impacts of SO2 and SO3 on Cu/zeolite SCR catalysts. Catalysis Today, 2010, 151, 266-270.	2.2	96
38	A Common Intermediate for N ₂ Formation in Enzymes and Zeolites: Sideâ€On Cu–Nitrosyl Complexes. Angewandte Chemie - International Edition, 2013, 52, 9985-9989.	7.2	94
39	Metal Carbonation of Forsterite in Supercritical CO ₂ and H ₂ O Using Solid State ²⁹ Si, ¹³ C NMR Spectroscopy. Journal of Physical Chemistry C, 2010, 114, 4126-4134.	1.5	89
40	Evolution of form in metal–organic frameworks. Nature Communications, 2017, 8, 14070.	5.8	89
41	Tomography and High-Resolution Electron Microscopy Study of Surfaces and Porosity in a Plate-like γ-Al ₂ O ₃ . Journal of Physical Chemistry C, 2013, 117, 179-186.	1.5	81
42	Changing Morphology of BaO/Al2O3during NO2Uptake and Release. Journal of Physical Chemistry B, 2005, 109, 7339-7344.	1.2	79
43	Understanding the nature of surface nitrates in BaO/ \hat{l}^3 -Al2O3 NOx storage materials: A combined experimental and theoretical study. Journal of Catalysis, 2009, 261, 17-22.	3.1	79
44	Magnetic mesoporous materials for removal of environmental wastes. Journal of Hazardous Materials, 2011, 192, 1140-1147.	6.5	78
45	Size-Dependent Catalytic Performance of CuO on γ-Al ₂ O ₃ : NO Reduction versus NH ₃ Oxidation. ACS Catalysis, 2012, 2, 1432-1440.	5.5	75
46	Structure of Î ⁻ Alumina: Toward the Atomic Level Understanding of Transition Alumina Phases. Journal of Physical Chemistry C, 2014, 118, 18051-18058.	1.5	72
47	Effects of Ba loading and calcination temperature on BaAl2O4 formation for BaO/Al2O3 NOx storage and reduction catalysts. Catalysis Today, 2006, 114, 86-93.	2.2	70
48	The adsorption of NO2and the NO + O2reaction on Na-Y,FAU: an in situ FTIR investigation. Physical Chemistry Chemical Physics, 2003, 5, 4045-4051.	1.3	68
49	The influence of the electrochemical stressing (potential step and potential-static holding) on the degradation of polymer electrolyte membrane fuel cell electrocatalysts. Journal of Power Sources, 2008, 185, 280-286.	4.0	67
50	Morphology-dependent phase transformation of \hat{I}^3 -Al2O3. Applied Catalysis A: General, 2015, 500, 58-68.	2.2	65
51	The Effect of Water on the Adsorption of NO2in Naâ~' and Baâ~'Y, FAU Zeolites:Â A Combined FTIR and TPD Investigation. Journal of Physical Chemistry B, 2004, 108, 3746-3753.	1.2	64
52	Single enzyme nanoparticles in nanoporous silica: A hierarchical approach to enzyme stabilization and immobilization. Enzyme and Microbial Technology, 2006, 39, 474-480.	1.6	63
53	Supported Pd nanoparticle catalysts with high activities and selectivities in liquid-phase furfural hydrogenation. Fuel, 2018, 226, 607-617.	3.4	60
54	CH ₄ Oxidation Activity in Pd and Pt–Pd Bimetallic Catalysts: Correlation with Surface PdO _{<i>x</i>} Quantified from the DRIFTS Study. ACS Catalysis, 2021, 11, 5894-5905.	5.5	59

#	Article	IF	CITATIONS
55	Direct propylene epoxidation with oxygen using a photo-electro-heterogeneous catalytic system. Nature Catalysis, 2022, 5, 37-44.	16.1	58
56	Controlling the acid-base properties of alumina for stable PtSn-based propane dehydrogenation catalysts. Applied Catalysis A: General, 2019, 572, 1-8.	2.2	57
57	Interaction of NO ₂ with BaO:  From Cooperative Adsorption to Ba(NO ₃) ₂ Formation. Journal of Physical Chemistry C, 2007, 111, 15299-15305.	1.5	56
58	Excellent sulfur resistance of Pt/BaO/CeO2 lean NOx trap catalysts. Applied Catalysis B: Environmental, 2008, 84, 545-551.	10.8	55
59	Dissecting the steps of CO ₂ reduction: 2. The interaction of CO and CO ₂ with Pd/l̂³-Al ₂ O ₃ : an in situ FTIR study. Physical Chemistry Chemical Physics, 2014, 16, 15126-15138.	1.3	51
60	High field 27Al MAS NMR and TPD studies of active sites in ethanol dehydration using thermally treated transitional aluminas as catalysts. Journal of Catalysis, 2016, 336, 85-93.	3.1	47
61	NO x uptake mechanism on Pt/BaO/Al2O3 catalysts. Catalysis Letters, 2006, 111, 119-126.	1.4	46
62	Magnetically-separable and highly-stable enzyme system based on crosslinked enzyme aggregates shipped in magnetite-coated mesoporous silica. Journal of Materials Chemistry, 2009, 19, 7864.	6.7	44
63	Morphology and size of Pt on Al2O3: The role of specific metal-support interactions between Pt and Al2O3. Journal of Catalysis, 2020, 385, 204-212.	3.1	44
64	Changes in Ba Phases in BaO/Al2O3 upon Thermal Aging and H2O Treatment. Catalysis Letters, 2005, 105, 259-268.	1.4	43
65	Synthesis of nanodispersed oxides of vanadium, titanium, molybdenum, and tungsten on mesoporous silica using atomic layer deposition. Topics in Catalysis, 2006, 39, 245-255.	1.3	43
66	Solid-State Hydriding Mechanism in the LiBH ₄ + MgH ₂ System. Journal of Physical Chemistry C, 2010, 114, 8089-8098.	1.5	43
67	Cu2O(100) surface as an active site for catalytic furfural hydrogenation. Applied Catalysis B: Environmental, 2021, 282, 119576.	10.8	43
68	Characterization of Dispersed Heteropoly Acid on Mesoporous Zeolite Using Solid-State ³¹ P NMR Spinâ^'Lattice Relaxation. Journal of the American Chemical Society, 2009, 131, 9715-9721.	6.6	42
69	Non-thermal plasma-assisted NOx reduction over alkali and alkaline earth ion exchanged Y, FAU zeolites. Catalysis Today, 2004, 89, 135-141.	2.2	41
70	A new class of highly dispersed VOx catalysts on mesoporous silica: Synthesis, characterization, and catalytic activity in the partial oxidation of ethanol. Applied Catalysis A: General, 2006, 300, 109-119.	2.2	41
71	Facile Synthesis and Characterization of Nanostructured Transition Metal/Ceria Solid Solutions (TM _{<i>x</i>} Ce _{1–<i>x</i>} O _{2â²l´} , TM = Mn, Ni, Co, or Fe) for CO Oxidation. Chemistry of Materials, 2017, 29, 2874-2882.	3.2	40
72	Ni catalysts for dry methane reforming prepared by A-site exsolution on mesoporous defect spinel magnesium aluminate. Applied Catalysis A: General, 2020, 602, 117694.	2.2	40

#	Article	IF	CITATIONS
73	Water-induced bulk Ba(NO3)2 formation from NO2 exposed thermally aged BaO/Al2O3. Applied Catalysis B: Environmental, 2007, 72, 233-239.	10.8	39
74	Inverse Temperature-Dependent Pathway of Cellulose Decrystallization in Trifluoroacetic Acid. Journal of Physical Chemistry B, 2007, 111, 5295-5300.	1.2	38
75	Molecular Active Sites in Heterogeneous Ir–La/C-Catalyzed Carbonylation of Methanol to Acetates. Journal of Physical Chemistry Letters, 2014, 5, 566-572.	2.1	38
76	Acid-base properties of Al2O3: Effects of morphology, crystalline phase, and additives. Journal of Catalysis, 2017, 345, 135-148.	3.1	38
77	Using a Surface-Sensitive Chemical Probe and a Bulk Structure Technique to Monitor the γ- to Î-Al ₂ O ₃ Phase Transformation. Journal of Physical Chemistry C, 2011, 115, 12575-12579.	1.5	37
78	Mesoporous mixed CuCo oxides as robust catalysts for liquid-phase furfural hydrogenation. Applied Catalysis A: General, 2019, 571, 118-126.	2.2	37
79	Nonthermal plasma-assisted catalytic NOx reduction over Ba-Y,FAU: the effect of catalyst preparation. Journal of Catalysis, 2003, 220, 291-298.	3.1	36
80	Oxidation of ethanol to acetaldehyde over Na-promoted vanadium oxide catalysts. Applied Catalysis A: General, 2007, 332, 263-272.	2.2	36
81	Cation Movements during Dehydration and NO ₂ Desorption in a Ba–Y,FAU Zeolite: An in Situ Time-Resolved X-ray Diffraction Study. Journal of Physical Chemistry C, 2013, 117, 3915-3922.	1.5	36
82	Water-Induced Morphology Changes in BaO/γ-Al2O3NOxStorage Materials:  an FTIR, TPD, and Time-Resolved Synchrotron XRD Study. Journal of Physical Chemistry C, 2007, 111, 4678-4687.	1.5	35
83	NMR studies of Cu/zeolite SCR catalysts hydrothermally aged with urea. Catalysis Today, 2008, 136, 34-39.	2.2	35
84	Possible origin of improved high temperature performance of hydrothermally aged Cu/beta zeolite catalysts. Catalysis Today, 2012, 184, 245-251.	2.2	35
85	Effect of Pt pre-sintering on the durability of PtPd/Al2O3 catalysts for CH4 oxidation. Applied Catalysis B: Environmental, 2020, 260, 118098.	10.8	34
86	Surface Density Dependent Catalytic Activity of Single Palladium Atoms Supported on Ceria**. Angewandte Chemie - International Edition, 2021, 60, 22769-22775.	7.2	34
87	Line narrowing in 1H MAS spectrum of mesoporous silica by removing adsorbed H2O using N2. Solid State Nuclear Magnetic Resonance, 2005, 27, 200-205.	1.5	32
88	Understanding Practical Catalysts Using a Surface Science Approach:  The Importance of Strong Interaction between BaO and Al ₂ O ₃ in NO <i>_x</i> Storage Materials. Journal of Physical Chemistry C, 2007, 111, 14942-14944.	1.5	32
89	Critical role of (100) facets on γ-Al2O3 for ethanol dehydration: Combined efforts of morphology-controlled synthesis and TEM study. Applied Catalysis A: General, 2018, 556, 121-128.	2.2	32
90	Efficient CO Oxidation by 50-Facet Cu ₂ 0 Nanocrystals Coated with CuO Nanoparticles. ACS Applied Materials & Interfaces, 2017, 9, 2495-2499.	4.0	31

#	Article	IF	CITATIONS
91	Effect of Barium Loading on the Desulfation of Pt-BaO/Al2O3Studied by H2TPRX, TEM, Sulfur K-edge XANES, and in Situ TR-XRD. Journal of Physical Chemistry B, 2006, 110, 10441-10448.	1.2	30
92	The Origin of Regioselectivity in 2â€Butanol Dehydration on Solid Acid Catalysts. ChemCatChem, 2011, 3, 1557-1561.	1.8	30
93	Adsorption and Formation of BaO Overlayers on γ-Al ₂ O ₃ Surfaces. Journal of Physical Chemistry C, 2008, 112, 18050-18060.	1.5	29
94	Studies of the Active Sites for Methane Dehydroaromatization Using Ultrahigh-Field Solid-State 95Mo NMR Spectroscopy. Journal of Physical Chemistry C, 2009, 113, 2936-2942.	1.5	29
95	Effect of number and properties of specific sites on alumina surfaces for Pt-Al2O3 catalysts. Applied Catalysis A: General, 2019, 569, 8-19.	2.2	29
96	High-Field One-Dimensional and Two-Dimensional ²⁷ Al Magic-Angle Spinning Nuclear Magnetic Resonance Study of Î,-, Î'-, and γ-Al ₂ O ₃ Dominated Aluminum Oxides: Toward Understanding the Al Sites in γ-Al ₂ O ₃ . ACS Omega, 2021, 6, 4090-4099.	1.6	29
97	Photo-catalytic oxidation of acetone on a TiO2 powder: An in situ FTIR investigation. Journal of Molecular Catalysis A, 2015, 406, 213-223.	4.8	28
98	NOx uptake on alkaline earth oxides (BaO, MgO, CaO and SrO) supported on γ-Al2O3. Catalysis Today, 2008, 136, 121-127.	2.2	27
99	Study the effects of mechanical activation on Li–N–H systems with 1H and 6Li solid-state NMR. Journal of Power Sources, 2007, 170, 419-424.	4.0	26
100	Probing the reaction pathway of dehydrogenation of the LiNH2+LiH mixture using in situ 1H NMR spectroscopy. Journal of Power Sources, 2008, 181, 116-119.	4.0	25
101	Characterization of Fe ²⁺ ions in Fe,H/SSZ-13 zeolites: FTIR spectroscopy of CO and NO probe molecules. Physical Chemistry Chemical Physics, 2016, 18, 10473-10485.	1.3	25
102	Effects of Novel Supports on the Physical and Catalytic Properties of Tungstophosphoric Acid for Alcohol Dehydration Reactions. Topics in Catalysis, 2008, 49, 259-267.	1.3	24
103	Ethanol dehydration on Î ³ -Al2O3: Effects of partial pressure and temperature. Molecular Catalysis, 2017, 434, 39-48.	1.0	24
104	Direct observation of ion exchange in mechanically activated LiH+MgB2 system using ultrahigh field nuclear magnetic resonance spectroscopy. Applied Physics Letters, 2009, 94, 141905.	1.5	22
105	Highly Dispersed and Active ReO _{<i>x</i>} on Alumina-Modified SBA-15 Silica for 2-Butanol Dehydration. ACS Catalysis, 2012, 2, 1020-1026.	5.5	22
106	Structure-dependent catalytic properties of mesoporous cobalt oxides in furfural hydrogenation. Applied Catalysis A: General, 2019, 583, 117125.	2.2	22
107	A large sample volume magic angle spinning nuclear magnetic resonance probe for in situ investigations with constant flow of reactants. Physical Chemistry Chemical Physics, 2012, 14, 2137-2143.	1.3	20
108	N–H and S–H insertions over Cu(I)-zeolites as heterogeneous catalysts. Journal of Molecular Catalysis A, 2016, 417, 10-18.	4.8	20

#	Article	IF	CITATIONS
109	Characterization of NOx species in dehydrated and hydrated Na- and Ba-Y, FAU zeolites formed in NO2 adsorption. Journal of Electron Spectroscopy and Related Phenomena, 2006, 150, 164-170.	0.8	19
110	Non-thermal Plasma-assisted NOx Reduction over Na-Y Zeolites: The Promotional Effect of Acid Sites. Catalysis Letters, 2006, 109, 1-6.	1.4	19
111	SiO2@V2O5@Al2O3 core–shell catalysts with high activity and stability for methane oxidation to formaldehyde. Journal of Catalysis, 2018, 368, 134-144.	3.1	19
112	Adsorption, Coadsorption, and Reaction of Acetaldehyde and NO2on Naâ^'Y,FAU:Â An In Situ FTIR Investigation. Journal of Physical Chemistry B, 2004, 108, 17050-17058.	1.2	18
113	Investigation of mechanical activation on Li–N–H systems using 6Li magic angle spinning nuclear magnetic resonance at ultra-high field. Journal of Power Sources, 2008, 182, 278-283.	4.0	18
114	A New Route to Improved Glucose Yields in Cellulose Hydrolysis. Journal of Biobased Materials and Bioenergy, 2007, 1, 210-214.	0.1	18
115	Roles of Pt and BaO in the Sulfation of Pt/BaO/Al ₂ O ₃ Lean NO <i>_x</i> Trap Materials:  Sulfur K-edge XANES and Pt L _{III} XAFS Studies. Journal of Physical Chemistry C, 2008, 112, 2981-2987.	1.5	17
116	Effects of Sulfation Level on the Desulfation Behavior of Presulfated Pt-BaO/Al ₂ O ₃ Lean NO <i>_x</i> Trap Catalysts: A Combined H ₂ Temperature-Programmed Reaction, in Situ Sulfur K-Edge X-ray Absorption Near-Edge Spectroscopy, X-ray Photoelectron Spectroscopy, and Time-Resolved X-ray Diffraction Study. Journal	1.5	17
117	of Physical Chemistry C, 2009, 113, 7336-7341. Detailed investigation of ion exchange in ball-milled LiH+MgB2 system using ultra-high field nuclear magnetic resonance spectroscopy. Journal of Power Sources, 2010, 195, 3645-3648.	4.0	16
118	Modification of the acid/base properties of γ-Al2O3 by oxide additives: An ethanol TPD investigation. Catalysis Today, 2016, 265, 240-244.	2.2	16
119	Acidic effect of porous alumina as supports for Pt nanoparticle catalysts in n-hexane reforming. Catalysis Science and Technology, 2018, 8, 3295-3303.	2.1	16
120	Characteristics of Desulfation Behavior for Presulfated Pt-BaO/CeO2 Lean NOx Trap Catalyst: The Role of the CeO2 Support. Journal of Physical Chemistry C, 2009, 113, 21123-21129.	1.5	14
121	Promotional Effects of H2O Treatment on NO x Storage Over Fresh and Thermally Aged Pt–BaO/Al2O3 Lean NO x Trap Catalysts. Catalysis Letters, 2008, 124, 39-45.	1.4	13
122	Template free facile synthesis of mesoporous mordenite for bulky molecular catalytic reactions. Journal of Industrial and Engineering Chemistry, 2018, 57, 363-369.	2.9	13
123	Morphology change and phase transformation of alumina related to defect sites and its use in catalyst preparation. Catalysis Today, 2020, 352, 323-328.	2.2	13
124	Interfacial effect of Pd supported on mesoporous oxide for catalytic furfural hydrogenation. Catalysis Today, 2021, 365, 291-300.	2.2	13
125	129Xe Nuclear magnetic resonance study on a solid-state defect in HZSM-5 zeolite. Microporous Materials, 1995, 4, 59-64.	1.6	12
126	Enhanced High Temperature Performance of MgAl2O4-Supported Pt–BaO Lean NOx Trap Catalysts. Topics in Catalysis, 2012, 55, 70-77.	1.3	12

#	Article	IF	CITATIONS
127	A new synthesis procedure for titanium-containing zeolites under strong alkaline conditions and the catalytic activity for partial oxidation and photocatalytic decomposition. Catalysis Letters, 1996, 37, 217-221.	1.4	11
128	Characterizing Surface Acidic Sites in Mesoporous-Silica-Supported Tungsten Oxide Catalysts Using Solid-State NMR and Quantum Chemistry Calculations. Journal of Physical Chemistry C, 2011, 115, 23354-23362.	1.5	11
129	Efficient copper catalysts for C H bond arylation under microwave heating: Direct access to multi-substituted pivanilides. Catalysis Communications, 2017, 90, 83-86.	1.6	11
130	Sequential high temperature reduction, low temperature hydrolysis for the regeneration of sulfated NOx trap catalysts. Catalysis Today, 2008, 136, 183-187.	2.2	10
131	Characterization of surface and bulk nitrates of γ-Al2O3–supported alkaline earth oxides using density functional theory. Physical Chemistry Chemical Physics, 2009, 11, 3380.	1.3	10
132	The Catalytic Chemistry of HCN + NO2over Naâ^' and Baâ^'Y,FAU:Â An in Situ FTIR and TPD/TPR Study. Journal of Physical Chemistry B, 2005, 109, 1481-1490.	1.2	9
133	Catalyst size and morphological effects on the interaction of NO2 with BaO/γ-Al2O3 materials. Catalysis Today, 2010, 151, 304-313.	2.2	8
134	Understanding Automotive Exhaust Catalysts Using a Surface Science Approach: Model NOx Storage Materials. Topics in Catalysis, 2013, 56, 1420-1440.	1.3	8
135	Pd/SiO2 as an active and durable CH4 oxidation catalyst for vehicle applications. Journal of Industrial and Engineering Chemistry, 2021, 99, 90-97.	2.9	7
136	Characterization of MoAl2O3 sol-gel catalyst by 27Al nuclear magnetic resonance spectroscopy. Journal of Molecular Catalysis A, 1996, 104, 285-291.	4.8	5
137	CH bond arylation of anilides inside copper-exchanged zeolites. Journal of Molecular Catalysis A, 2016, 417, 64-70.	4.8	5
138	Molecular Engineered Safer Organic Battery through the Incorporation of Flame Retarding Organophosphonate Moiety. ACS Applied Materials & Interfaces, 2018, 10, 10096-10101.	4.0	5
139	Key Role of aâ€Top CO on Terrace Sites of Metallic Pd Clusters for CO Oxidation. Chemistry - A European Journal, 2022, 28, .	1.7	5
140	Effect of reductive treatments on Pt behavior and NOx storage in lean NOx trap catalysts. Catalysis Today, 2011, 175, 78-82.	2.2	4
141	Promotional Effect of CO2 on Desulfation Processes for Pre-Sulfated Pt-BaO/Al2O3 Lean NOx Trap Catalysts. Topics in Catalysis, 2009, 52, 1719-1722.	1.3	3
142	Mechanism of CO Oxidation on Pd/CeO 2 (100): The Unique Surfaceâ€ S tructure of CeO 2 (100) and the Role of Peroxide. ChemCatChem, 2020, 12, 5164-5172.	1.8	3
143	Rücktitelbild: Surface Density Dependent Catalytic Activity of Single Palladium Atoms Supported on Ceria (Angew. Chem. 42/2021). Angewandte Chemie, 2021, 133, 23212-23212.	1.6	1
144	Surface Density Dependent Catalytic Activity of Single Palladium Atoms Supported on Ceria**. Angewandte Chemie, 2021, 133, 22951.	1.6	0